energies

MDPI

Article

Effect of Salts on Interfacial Tension and CO_2 Mass Transfer in Carbonated Water Injection

Aly A Hamouda * and Nikhil Bagalkot

Department of Petroleum Technology, University of Stavanger, Stavanger 4035, Norway; nikhil.bagalkot@uis.no
* Correspondence: aly.hamouda@uis.no; Tel.: +47-5183-2271

Received: 1 February 2019; Accepted: 22 February 2019; Published: 24 February 2019

Abstract: Carbonated water injection (CWI) is a promising enhanced oil recovery (EOR) and CO_2 sequestration method, which overcomes the problems associated with CO_2 EOR. CO_2 mass transfer and interfacial tension (IFT) are important parameters that influence oil recovery efficiency. This study addresses the impact of $MgCl_2$ and Na_2SO_4 in carbonated water (CW) on CW/hydrocarbon IFT and CO_2 mass transfer. An axisymmetric drop shape analysis was used to estimate the IFT and the CO_2 diffusion coefficient. It was found that CW+$MgCl_2$ reduced both the CW/n-decane IFT (36.5%) and CO_2 mass transfer, while CW+Na_2SO_4 increased both the IFT and CO_2 mass transfer (57%). It is suggested that reduction in IFT for CW+$MgCl_2$ brine is mainly due to the higher hydration energy of Mg^{2+}. The Mg^{2+} ion forms a tight bond to the first hydration shell $[Mg(H_2O)_6]^{2+}$, this increases the effective size at the interface, hence reduce IFT. Meanwhile, the $SO_4{}^{2-}$ outer hydration shell has free OH groups, which may locally promote CO_2 mass transfer. The study illustrates the potential of combining salts and CW in enhancing CO_2 mass transfer that can be the base for further investigations. Furthermore, the contribution and proposed mechanisms of the different ions ($SO_4{}^{2-}$ and Mg^{2+}) to the physical process in carbonated water/hydrocarbon have been addressed, which forms one of primary bases of EOR.

Keywords: CO_2+brine; interfacial tension; carbonated water; CO_2 diffusion coefficient; synthetic sea water

1. Introduction

Recent years have seen an increased interest in carbonated water injection (CWI) as secondary/tertiary enhanced oil recovery (EOR) method. CWI has been projected as a substitute to the CO_2 EOR to overcome challenges such as poor sweep efficiency, and early breakthrough [1]. Low sweep efficiency associated with CO_2 EOR due to gravity segregation and capillary instabilities causes mobility issues [1,2]. For CWI, the CO_2 is dissolved in water and has higher density; this reduces gravity segregation, thereby improving the sweep efficiency. Furthermore, for CWI, an increased mobility of oil is observed as a result of a reduction in the viscosity of the oil resulting from the dissolution/diffusion of CO_2, which enhances sweep efficiency [2]. Figure 1 (inspired from [2]) shows the pictorial representation between the comparison between CO_2 EOR and CWI regarding sweep efficiency and sweep profile. Another problem with CO_2 EOR is that in many of the cases, CO_2 is not readily available in the required volumes. Thus, the transportation of CO_2 becomes necessary, which increases the use costs. CWI, which requires less CO_2, partially reduces the costs associated with transport. CWI is also of interest due to its capability of coupling oil recovery and CO_2 sequestration. Dissolved CO_2 in water (carbonated water) has higher density compared to native brine (formation water). Hence, it sinks into the bottom of the reservoir, eliminating the risk of buoyancy-driven leakage of CO_2 [3–6], thus improving CO_2 sequestration capability.

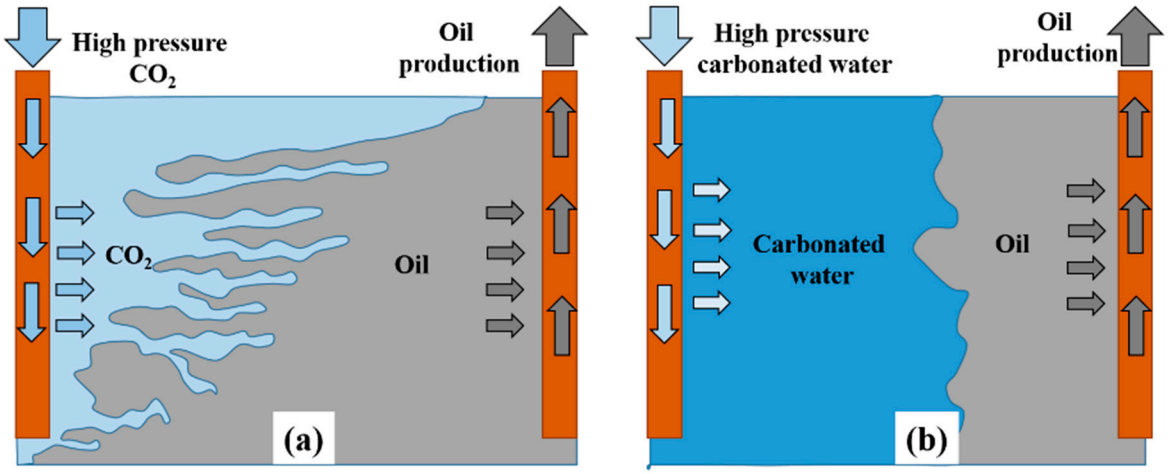

Figure 1. Pictorial representation of sweep front for the case of (**a**) CO_2 flooding and (**b**) Carbonated water injection.

At pore scale, the rock wettability defined by rock-fluid interaction, capillary pressure through interfacial tension (IFT), and swelling and mobility through CO_2 mass transfer (oil-CW interaction) are the primary mechanisms responsible for governing the oil recovery by CWI. Various ways have been described in the literature (nanofluid, microbial, polymer, and salts) to address the fluid-fluid and fluid-rock interactions as EOR methods. Lately more attention has been directed to low-salinity water studies [7,8], which indicated wettability and interfacial alteration. The potential of saline water to change the wettability of the rock has been well established [9,10], and has been extended to CWI by Manshad, et al. [11]. Previous studies [9,11–13] have presented extensive data on the IFT between brine/hydrocarbon and a few studies [7,14] have also been dedicated to carbonated brine/hydrocarbon [15]. Table 1 gives a summary of work done in the literature on the effect of salts on IFT. Table 1 has been divided into different sections (increasing IFT, decreasing IFT, salt-dependent IFT variation, and IFT of carbonated brine/hydrocarbon systems) depending on the investigations made by the various studies. It may be observed from Table 1 that there are controversial trends of the IFT trend. For example Gomari and Hamouda [9] and Serrano-Saldaña, et al. [16] showed that salts reduced the IFT. However, Ikeda, et al. [17] and Cai, et al. [12] observed that salts increased the IFT. Furthermore, Aveyard and Saleem [18] and Lashkarbolooki, et al. [19] have observed both an increase and decrease in IFT, and concluded that the variation of IFT is a function of the composition of the brine. Additionally, the increase or decrease in IFT was also found to be the function of concentration of salt [16,20]. Not all the salts will have same effect on the IFT; there may be certain types of salts which would have more prominent effects on reducing the IFT than others. Gomari and Hamouda [9], Hosseini, et al. [20], and Lashkarbolooki, et al. [19] observed that $MgCl_2$ specifically Mg^{2+} ions leads to lower IFT compared to other salts or ions present in their study. Aveyard and Saleem [18] showed that out of seven different salts only KI was able to lower the IFT of n-dodecane and n-decane/brine while other lead to an increase in IFT. Cai, et al. [12] observed the IFT of normal alkane+brine is weakly dependent on slat species. Therefore, there is a contrasting observation for IFT. Hence, there is a need for further investigations. For CW+salt/hydrocarbon system, there are a limited number of studies available [7,14]. Unfortunately, there is insufficient data to understand the critical interfacial phenomena occurring between brine CW/hydrocarbon. This has motivated this work to thoroughly investigate the influence of salts on the CW/hydrocarbon interfacial tension.

Table 1. IFT obtained by different studies for brine/hydrocarbon and carbonated brine/hydrocarbon systems.

References	Type of Aqueous Systems	Experimental Conditions	Observations
Reduction in IFT			
Gomari and Hamouda [9]	n-decane/brine with $MgCl_2$ and Na_2SO_4	82.4 to 158 °C, atmospheric pressure	IFT reduction in the presence of $MgCl_2$ and Na_2SO_4 compared to distilled water
Serrano-Saldaña, et al. [16]	n-dodecane/brine with sodium dodecyl sulfate (SDS) and NaCl	25 °C, atmospheric pressure	The presence and rising surfactant concentration leads to a reduction in the IFT
Hosseini, et al. [20]	Crude oil/brine with Na^+, K^+, Cl, Mg^{2+}, and Ca^{2+} ions	25 °C, atmospheric pressure	The presence of divalent ions (Ca^{2+} and Mg^{2+}) decreases the oil/brine IFT. At a given concentration Mg^{2+} shows a lower oil/brine IFT than Ca^{2+}
Increment in IFT			
Ikeda, et al. [17]	n-hexane/water with NaCl	25 °C, 0 to 100 Mpa	Increment in IFT due to the presence of NaCl in water
Cai, et al. [13]	normal alkane + water/brine with NaCl, $CaCl_2$, $MgCl_2$	25 to 80 °C,1 to 300 bar	Increase in IFT due to the presence of salt. Weakly dependent on pressure and salt species
Badakshan and Bakes [21]	Toluene, n-hexane and cyclohexane/brine with NaCl, $NaHCO_3$, Na_2SO_4	20 °C to 75 °C, atmospheric pressure	For all the salts an increment in IFT was observed
Salt-dependent IFT variation			
Lashkarbolooki, et al. [19]	Crude oil/brine with NaCl, KCl, Na_2SO_4, $MgSO_4$, $CaSO_4$, $CaCl_2$, and $MgCl_2$	Ambient temperature and pressure	Reduction in IFT at high salinity conditions especially for $MgCl_2$. The increment in IFT for monovalent salts such as NaCl and KCl is used
Aveyard and Saleem [18]	n-dodecane-decane/brine with LiCl, NaCl, KCl, KBr, NaBr, KI, and Na_2SO_4	20 °C, atmospheric pressure	Reduction in IFT in the presence of KI. An increment in IFT for rest of the salts
IFT of carbonated brine/hydrocarbon system			
Manshad, et al. [15]	Crude oil/carbonated water with NaCl, $CaCl_2$, $MgCl_2$, KCl, and Na_2SO_4	75 °C, pressure up to 137 bar	Presence of salt reduces the IFT and is a function of the type of salt
Nowrouzi, et al. [7]	Crude oil/ carbonated brine with NaCl, $CaCl_2$, $MgCl_2$, KCl, $MgSO_4$, K_2SO_4, and Na_2SO_4	75 °C, up to 140 bar	Salts are able to reduce the IFT. Addition of CO_2 further enhances the reduction in IFT. Minimum IFT was obtained for $MgCl_2$+K_2SO_4 combination
Isdahl [21]	n-decane/ carbonated synthetic sea water with silica nanofluid	25 °C and 45 °C, 10 to 90 bar	Marginal reduction in IFT for the combination of salt and CO_2 in water

The mass transfer of CO_2 and the resulting mechanisms, such as swelling and enhanced mobility of the oil, dictate the degree of oil recovery in CO_2-based EOR methods [4,22]. From the above discussion and Table 1 it may be said that thus far, most of the studies have concentrated on examining interfacial and wettability aspects of CO_2/oil, CW/oil, water/oil, and carbonated smart water/oil systems. However, there is a lack of understanding of CO_2 mass transfer, and factors influencing CO_2 mass transfer, especially when it comes to CW/hydrocarbon systems. The diffusive mass transfer of gases, especially CO_2 into oil, is of primary importance when it comes to CO_2 and CW flooding. Diffusion of CO_2 into oil results in the reduction of viscosity, and displacement of oil (including heavy oil) from reservoirs to surface. Few studies have looked into the aspect of CO_2 mass transfer, and most of these studies are related to CO_2/hydrocarbon [23–25] or CO_2/water [26] systems. The number of studies diminishes when it comes to CW/hydrocarbon systems [27]. Furthermore, there may be a significant neglect of the application of salts as a CO_2 mass transfer enhancement tool for CW/hydrocarbon system. Zhu, et al. [28] in their study on syngas and fermentation have experimentally shown that salts in water may enhance mass transfer of gas in water. Zhu, et al. [28] showed that the ions of dissolved salts in water stopped the coalesces of CO bubbles, thereby increasing the surface area between CO and water. Collins [29] showed that salts in water increased the entropy of the solution, which enhances the mobility leading to a convective movement in bulk liquid, and may

enhance the mass transfer. Conventionally, salts in water have been viewed as wettability and IFT modifiers; however, salts may have more valuable potential and may also be used as CO_2 mass transfer enhancement tool, and this widens the scope of applicability of salts. Therefore, investigations are needed to establish if salts can improve the CO_2 mass transfer in CW/hydrocarbon systems.

Previous studies have developed various methods to understand the CO_2 mass transfer by estimating the diffusion coefficient of CO_2 in bulk liquids. These methods may be put into two groups, compositional analysis [30,31], and pressure decay [32,33] methods. In compositional analysis, errors will be caused in the extraction of the sample from the setup and carrying out gas chromatography, especially at high pressures and temperatures, which may affect the estimation of the diffusion coefficient [25]. Furthermore, the compositional method is time-consuming, complicated, and expensive [34]. The pressure decay method solves the problems associated with the compositional analysis. However, it requires long experimental time (20–100 h or more). Additionally, the diffusion coefficient obtained by pressure decay method is not for a particular pressure but a range of pressures [25,35]. Hence, there is a requirement for a well-established, reliable, quicker, and simple method for estimating the diffusion coefficient of CO_2 in hydrocarbon, which may be used for both gas-liquid and liquid-liquid systems. Of late, Axisymmetric Drop Shape Analysis (ADSA) using pendant drop equipment coupled with a computational scheme has been used to estimate the diffusion coefficient of gases into liquids [23,24]. The experiments using ADSA can be carried out at high temperature and pressure (up to 60 MPa and 180 °C) [27]. Furthermore, unlike the pressure decay method, the experiments using the ADSA pendant drop technique can be carried out at isothermal and isobaric conditions. The flexibility, simplicity, lesser time, and no human interference makes the ADSA method suitable for calculating the diffusion coefficient of gases into the bulk liquids. The ADSA pendant drop technique is also widely used to estimate the IFT between two fluid at elevated pressure and temperature [36]. The ADSA method has an accuracy of ± 0.05 mN/m^2 when estimating the IFT [36,37]. Therefore, by using the ADSA method, both mass transfer and interfacial studies may be carried out using the same experimental setup and with higher accuracy.

From the above discussion on literature studies, two crucial points may be made. First, the studies and knowledge of the influence of salts on the CW/hydrocarbon IFT are insufficient. Dynamic IFT analysis has been entirely neglected, and there are some opposing trends on the influence of salts on brine/hydrocarbon IFT. Second and importantly, there is significant overlooking of the effects of salts on CO_2 mass transfer. Therefore, there is a lack of understanding of CO_2 mass transfer, and factors influencing CO_2 mass transfer, especially when it comes to CW/hydrocarbon systems. The present work tries to address these issues. As a result, the objective of the present study is to investigate the impact of salts in CW, particularly Na_2SO_4 and $MgCl_2$ in altering the CW/hydrocarbon IFT and enhancing the CO_2 mass transfer. In fulfilling these objectives, the study adds four major contributions to the existing knowledge of CW/hydrocarbon systems. First, the experiments were designed to analyze both dynamic and equilibrium IFT, and simultaneously carry out mass transfer studies. Second, the experimental pressure range (50–100 bar) was chosen to study the influence of the phase of both gaseous and supercritical phase of CO_2 on the mass transfer and IFT. Third, to the best of authors knowledge, this would be the first time the impact of salts on the CW/hydrocarbon as a combined mechanism of IFT and the mass transfer enhancement tool will be addressed. Fourth, a relatively new and advanced numerical model, which couples with experimental results to estimate the CO_2 diffusion coefficient at-large range of pressure and temperate, has been developed. The present study, through experimental, theoretical, and numerical models, analyzes the influence of salts on the interfacial and mass transfer aspects of CW/hydrocarbon system. ADSA pendant drop experiments have been carried out for a pressure range of 50–100 bar at 45 °C. The study will focus on the effect of $MgCl_2$ and Na_2SO_4 on IFT and diffusion coefficient.

2. Experimental and Numerical Study

Figure 2a shows the cross-section of the see-through high-pressure cell (PVT cell) where the experiments were carried out. The pendant hydrocarbon drop (HD) consisting of n-decane will be known as drop phase, and the drop phase is surrounded by environmental fluid consisting of salts dissolved in carbonated water known as carbonated brine (CB). The mass of the CO_2 in the brine surrounding the drop phase is always monitored and maintained at the saturation limit. The solubility of CO_2 is higher in hydrocarbons compared to water or brine; therefore, when the hydrocarbon contacts the CB, the CO_2 from the CB diffuses into the drop phase. The resulting mass transfer of CO_2 is driven by the concentration gradient between the drop phase and the environmental fluid. The mass transfer of CO_2 depends on the IFT, CO_2 solubility, density gradient, and experimental conditions. When salts are dissolved in water, they release ions. Depending on the type of salts these ions may be surface active or interface repelling. The ions are responsible for altering the IFT of the CW/oil system. Since salts in water can alter the IFT, there may be a possibility that they may also influence the mass transfer occurring across the interface.

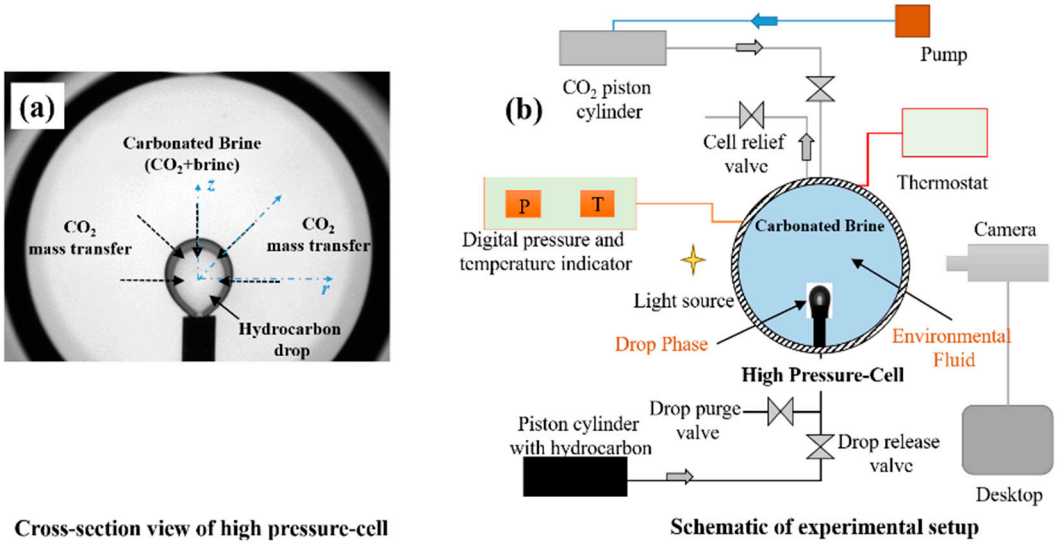

Figure 2. (**a**) Cross-section view of the PVT cell; (**b**) Schematics of the experimental setup.

2.1. Materials

The n-decane light hydrocarbon forms the pendant drop phase (Merck KGaA (purity 99%)). As discussed in the introduction, most studies fail to address fundamental phenomena such as CO_2 mass transfer, IFT, and hydrocarbon property alterations, which are critical in understanding and optimizing the process of recovery by CO_2-saturated water. Hence, the first step would be to start with light and homogeneous hydrocarbon. Once the knowledge of fundamental physics for CW-n-decane system has been acquired, then it would easy and meaningful to move to a more complex multicomponent hydrocarbons such as crude oil and synthetic oil. CO_2 with purity of 99.9% (PRAXAIR) was used to prepare the CW/CB. NaCl, $MgCl_2$, Na_2SO_4, $CaCl_2$, KCl, and $NaHCO_3$ salts were used to prepare the brine by dissolving them in deionized water (DIW). The composition of each of these was maintained according to the synthetic seawater (SSW) as given by Hamouda and Maevskiy [38]. The focus of the present study was to identify the feasibility of salts as IFT reduction and mass transfer enhancement option in a CW/hydrocarbon system. Therefore, only the composition of the brine has been altered, and the study of the influence of varying the concentration of salts has been left for future studies. SSW formed the base brine solution and out of this, four more brine types were created either by retaining only $MgCl_2$ (DIW+$MgCl_2$) and Na_2SO_4 (DIW+Na_2SO_4) or by removing $MgCl_2$ (SSW-$MgCl_2$) or Na_2SO_4 (SSW-Na_2SO_4). This variation in

brine composition was done to investigate the influence of Mg^{2+} and SO_4^{2-} ions on the IFT and CO_2 mass transfer. Table 2 gives the types of brine, compositions, and the purpose of forming each brine types. The brines presented in Table 2 will be saturated with CO_2, and from now on in this study, the combination of CO_2+SSW, which is carbonated SSW, will be abbreviated as C_{SSW}. Similarly, $C_{SSW\text{-}MgCl2}$ (CO_2+SSW-$MgCl_2$), $C_{SSW\text{-}Na2SO4}$ (CO_2+SSW-Na_2SO_4), CW_{+MgCl2} (CO_2+DIW+$MgCl_2$), and $CW_{+\ Na2SO4}$ (CO_2+DIW+Na_2SO_4). Collectively, the combination of CO_2+brines will be termed as CB in the present study. The fluid properties such as density and viscosity of water, CO_2, and n-decane at experimental pressure and temperatures, have been obtained from NIST Chemistry Web Book [39]. *Aqion* Version 6 software was used to obtain the pH of the each of these brines with and without CO_2, to which the concentration of salts in brine is provided as an input.

Table 2. Types of brine, compositions, and the purpose of forming each brine types.

Brine	Composition (g/L)						Purpose
	NaCl	$MgCl_2$ *$6H_2O$	Na_2SO_4	$CaCl_2$ *$2H_2O$	KCl	$NaHCO_3$	
SSW	23.38	9.05	3.41	1.91	0.75	0.17	Combination of salts on CO_2 mass transfer and IFT
SSW-$MgCl_2$	23.38	0	3.41	1.91	0.75	0.17	Combination of salts in the absence of Magnesium on IFT and CO_2 mass transfer
SSW-Na_2SO_4	23.38	9.05	0	1.91	0.75	0.17	Combination of salts in the absence of Sulfate on IFT and CO_2 mass transfer
DIW+$MgCl_2$	0	9.05	0	0	0	0	Magnesium on CO_2 mass transfer and IFT
DIW+$NaSO_4$	0	0	3.41	0	0	0	Sulfate on CO_2 mass transfer and IFT

2.2. Experimental Setup and Procedure

The equipment and design of the experimental setup are similar to that presented in Bagalkot and Hamouda [27]. The schematic of the experimental setup is shown in Figure 2b. The pendant drop equipment manufactured by EUROTHECHNICA and KRUSS consists of a cylindrical high-pressure cell (PVT cell). The PVT cell is see-through and placed between a high-resolution camera and light source. The capacity of PVT cell is 25 mL, and it can withstand a maximum pressure and temperature of 68.9 Mpa and 180 °C, respectively. A pump (maximum pressure of 32 MPa, GILSON) linked to a piston-cylinder containing CO_2 maintains the pressure in the PVT cell. Furthermore, details of the procedure and experimental setup may be obtained from Bagalkot and Hamouda [27]. Additional experiments were carried out using gas flow meter at 25 °C to estimate the saturation of CO_2 in brine at different pressures, and the result obtained was compared with the model presented by Duan and Sun [40]; there was a maximum error of 3% in the mass of CO_2. The experiments were carried out for a pressure range of 50 to 100 bar, at 45 °C. For these pressures and temperatures, CO_2 is in a gaseous state for P<74 bar at 45 °C and P>74 bar CO_2 is in the supercritical phase. Hence, the experiments will cover the effect of both gaseous and supercritical CO_2. Therefore, there may be a possibility of observing the behavior of various properties (IFT, CO_2 mass transfer, and diffusion coefficient) near to the phase change pressure of CO_2 (74 bar).

2.3. IFT Measurement

The dynamic and equilibrium IFT between CB/n-decane was measured using the ADSA method. The pendant drop method employed in the present study is a practical, accurate, and popular method to measure the IFT of the fluid-fluid system, the method applies Equation (1) to measure the IFT.

$$IFT = \frac{\Delta\rho g d^2}{B}, \quad (1)$$

where $\Delta\rho$ (kg/m^3) is the density difference between the drop and environmental phases; g (m/s^2) is the acceleration due to gravity, and d (m) is the maximum horizontal diameter of the unmagnified pendant drop. In Equation (1) three parameters are of significance, B, d, and $\Delta\rho$. Among these

B and *d* are calculated by the drop analysis software, while the densities of both drop phase and environmental phases must be input in the software. When the drop phase (HD, n-decane) contacts the CB, CO_2 diffuses from CB into the HD, which alters the HD density and viscosity. Therefore, for accurate measurement of IFT (dynamic and equilibrium), it is essential to know the density changes of the HD due to the CO_2 mass transfer. The present study adopts the dynamic and equilibrium IFT measuring technique developed by Bagalkot, et al. [41] for the fluid-fluid system. In case of the CO_2-hydrocarbon system, the measurement uncertainty is ± 0.3 mN/m. If water is present, uncertainties rise to ± 0.5 mN/m [42]. The uncertainty depends on the absolute value of the density difference and becomes greater as the density difference decreases [43].

2.4. Diffusion Coefficient Measurement

2.4.1. Mathematical Model

Molecular diffusion of CO_2 from CB or CW into hydrocarbon pendant drop is a concentration-driven process. In the present study, Fick's second law (Equation (2)) is employed to represent the diffusive mass transfer process of CO_2 across the interface. The pendant drop is symmetrical about the *z*-axis (Figure 2a). Therefore, it would be appropriate and convenient to adopt a cylindrical coordinate system (r, θ, z) rather than a Cartesian coordinate system (x, y, and z). Furthermore, details of the model, assumptions/limitations, and its boundary conditions for solving Equation (2) may be found in Bagalkot and Hamouda [27], Bagalkot and Hamouda [44], and Bagalkot and Hamouda [35].

$$\frac{\partial C}{\partial t} = D(t)\left\{\frac{1}{r}\frac{\partial C}{\partial r} + \frac{\partial^2 C}{\partial r^2} + \frac{\partial^2 C}{\partial z^2}\right\}, \tag{2}$$

In Equation (2), C is the concentration of CO_2 in the drop phase (kg/m^3), and $D(t)$ represents the diffusion coefficient (m^2/s). Equation (2) provides the spatial distribution of the concentration of CO_2 in the drop phase as a function of time. The diffusion of CO_2 from CW/CB into the hydrocarbon starts after the HD is formed. At the onset of the experiment ($t = 0$ s), the concentration of CO_2 in the pendant drop is zero at $t = 0$ (Equation (3)).

$$C(r, z, t = 0) = 0 \tag{3}$$

At thermodynamic equilibrium [45], CO_2 concentration at the interface remains constant as long as the pressure and temperature of the system are held constant. On this basis, Equation (4) represents the boundary condition at the interface.

$$C(r = R_D, z = R_D, t > 0) = C_o, \tag{4}$$

where R_D is the radius of the drop, and C_o is the concentration of CO_2 at the interface. A zero (constant) flux boundary condition is employed to address the continuity at the center of the drop ($r = 0$) (Equation (5)).

$$\frac{\partial C(r = 0, z, t)}{\partial r} = 0 \tag{5}$$

Equation (2) along with boundary and initial conditions (Equations (3)–(5)) are numerically solvable, to obtain the time and space-dependent concentration of CO_2 in the drop. The volumetric average of CO_2 concertation in the drop phase (C_{avg} (m^3)) is obtained from Equation (6) as a function of time.

$$C_{avg}(t) = \iint\limits_{(r,z)\in P_d} \frac{C(r, z)}{C_o} r dr dz \tag{6}$$

Furthermore, the parameter C_{avg} is used to calculate the swelling factor (*SF*) (Equation (7)), which is the ratio of the volume of the CO_2 saturated drop phase to the initial volume of drop phase.

$$SF = 1 + \frac{\int_0^T \frac{[V_{\exp}(t) - V_o] C_{avg}(t) dt}{V_{\exp}(t)^2}}{\int_0^T \frac{[C_{avg}{}^2(t)] dt}{V_{\exp}(t)^2}}, \quad (7)$$

In Equation (7), $V_{exp}(t)$ (m^3) is the experimentally obtained volume of drop phase at any instant t (s), and T (s) is the total experimental time; Vo (m^3) is the initial volume ($t = 0$) of the pendant drop obtained from experiments.

At each moment, the volume of the drop phase (HD) is the aggregate of the volume of the hydrocarbon in the drop phase (initial volume of drop) (V_o) and the increment in volume due to by the diffusion of CO_2 in the hydrocarbon (Equation (8)) [44]. The increment in volume is the product of C_{avg}, and *SF-1*.

$$V(t) = V_o + (SF - 1) \cdot C_{avg}(t) \quad (8)$$

An optimization function (*F*) (non-dimensional) as a function of the difference in the experimental ($V_{exp}(t)$) and numerical volume ($V(t)$) is used (Equation (8)) and the minimum of the optimization function (F_{min}) would give the diffusion coefficient of CO_2 in the hydrocarbon. The lower the F_{min}, the lower the error in estimating the diffusion coefficient compared to the experimental.

$$F = \sqrt{\frac{1}{T} \int_0^T \frac{[V_{\exp}(t) - V(t)]^2 dt}{V_{\exp}(t)^2}} * 100\% \quad (9)$$

2.4.2. Numerical Model

A semi-implicit finite difference numerical scheme was adopted to solve Equation (2) and obtain the CO_2 concentration profiles in the pendant drop. The model assumption/limitations, validation, and description may be found in Bagalkot and Hamouda [35].

2.4.3. Dynamic Interface (Boundary) Method

One of the significant and visible implications of CO_2 diffusion in hydrocarbon is the swelling or the increment in the volume of the hydrocarbon. Therefore, the volume of the pendant drop is not the same as that of initial time, and it increases with time. The increment in the volume indicates a change in the surface area at the CW/oil interface and hence, the movement of the fluid-fluid interface. However, most of the studies carrying out diffusion coefficient measurement using pendant drop experiment assume a quasi-static nature of the fluid-fluid interface, therefore neglecting increase in volume and thus displacement of the interface [25,46]. Such an assumption, especially for CW/oil system where there is a significant increment in volume, would lead to inaccuracy in estimating the diffusion coefficient. Bagalkot and Hamouda [27] showed that error due to the assumption of a static interface is approximately 2% at 10 bar to a significant 36% at 60 bar. Bagalkot and Hamouda [35] developed a simple and effective method to incorporate the dynamic nature of the CW-hydrocarbon interface (boundary). The current study extends the method to CB-hydrocarbon system.

3. Results and Conclusions

3.1. Swelling and Diffusion Coefficient

Figure 3 shows the mass of CO_2 transferred into the n-decane drop (CO_2 mole/ml volume of drop) from the surrounding CB (CW, $C_{SSW\text{-}MgCl2}$, $C_{SSW\text{-}Na2SO4}$, CW_{+MgCl2}, and $CW_{+Na2SO4}$) from the start

of the experiment until equilibrium is attained. The analysis has been carried out for 50 bar (3a), 70 bar (3b), 80 bar (3c), and 100 bar (3d) at 45 °C. For all the brine types and pressures, the CO_2 mass transfer with time may be divided into two regions. In the first region, the CO_2 mass transfer increases sharply, followed by the second region. In the second region the rate of mass transfer decreases and a plateau is reached, from where the mass transfer increase is negligible, and an equilibrium is approached. The first region of sharp increase takes a shorter time compared to the second region; however, a substantial CO_2 mass transfer occurs in the region of sharp increase. The sharp increase is followed by the gradual increase in mass transfer, which may be explained by the decrease in the CO_2 concentration gradient across the interface as CO_2 diffuses into the n-decane. It may be observed that there is a considerable variation in the profile and amount of mass transfer of CO_2 into n-decane among different brine compositions, indicating that the CO_2 mass transfer across the interface is sensitive to the composition of the brine. For the CBs $C_{SSW\text{-}MgCl2}$, C_{SSW}, and $CW_{+\,Na2SO4}$ there is a greater CO_2 mass transfer compared to the CW, while a lower CO_2 mass transfer is observed for $C_{SSW\text{-}Na2SO4}$ and CW_{+MgCl2} than CW. Furthermore, a largest CO_2 mass transfer is observed for brine $CW_{+Na2SO4}$, and the least mass transfer is observed for brine CW_{+MgCl2}. Therefore, it may be concluded that the combination of CW and Na_2SO_4 would assist the CO_2 mass transfer leading to a higher mass transfer of CO_2, while the CW and $MgCl_2$ combination does the opposite.

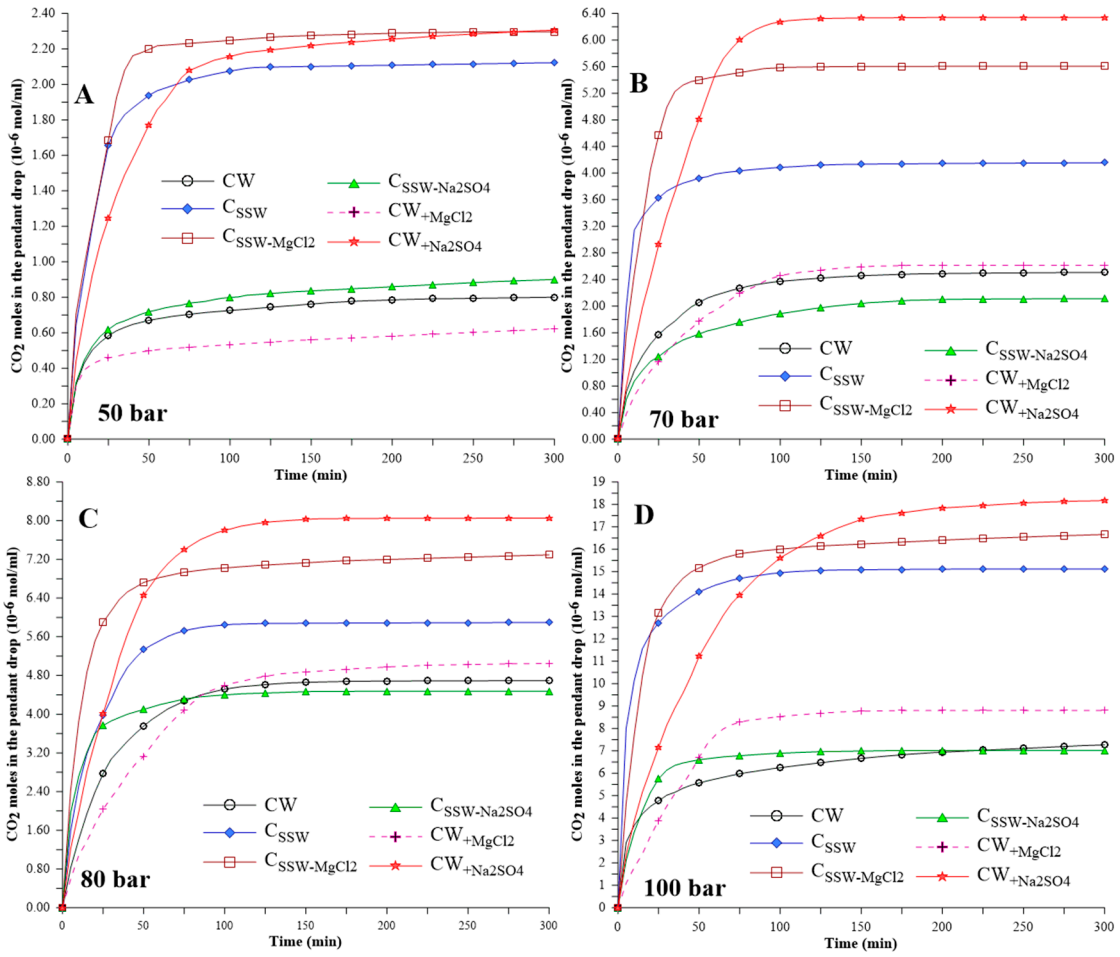

Figure 3. Mass of CO_2 transferred into the n-decane drop (mole/ml) from the start of the experiment till equilibrium for 50 bar (**a**), 70 bar (**b**), 80 bar (**c**), and 100 bar (**d**).

Figure 4 shows the swelling (ratio of equilibrium to initial volume) of the n-decane pendant drop due to the mass transfer of CO_2 for different CB (CW, C_{SSW}, $C_{SSW\text{-}MgCl2}$, $C_{SSW\text{-}Na2SO4}$, CW_{+MgCl2},

and $CW_{+Na2SO4}$) for a pressure range of 50-100 bar at temperature 45 °C. For a pure hydrocarbon+CO_2 system the higher the CO_2 mass transfer, the more significant will be the swelling of the hydrocarbon. Unsurprisingly, the swelling results in Figure 4 are analogous to the trend in Figure 3 (CO_2 mole). For example, in Figure 3, Na_2SO_4 enhances the CO_2 mass transfer. Therefore, in Figure 4 a larger swelling of drop phase (n-decane) is observed for cases where the brine consisted of Na_2SO_4, while a lower swelling of brine consisting of $MgCl_2$. Similar to CO_2 mass transfer (Figure 3), the combination of Na_2SO_4 and $MgCl_2$ resulted in an intermediate swelling.

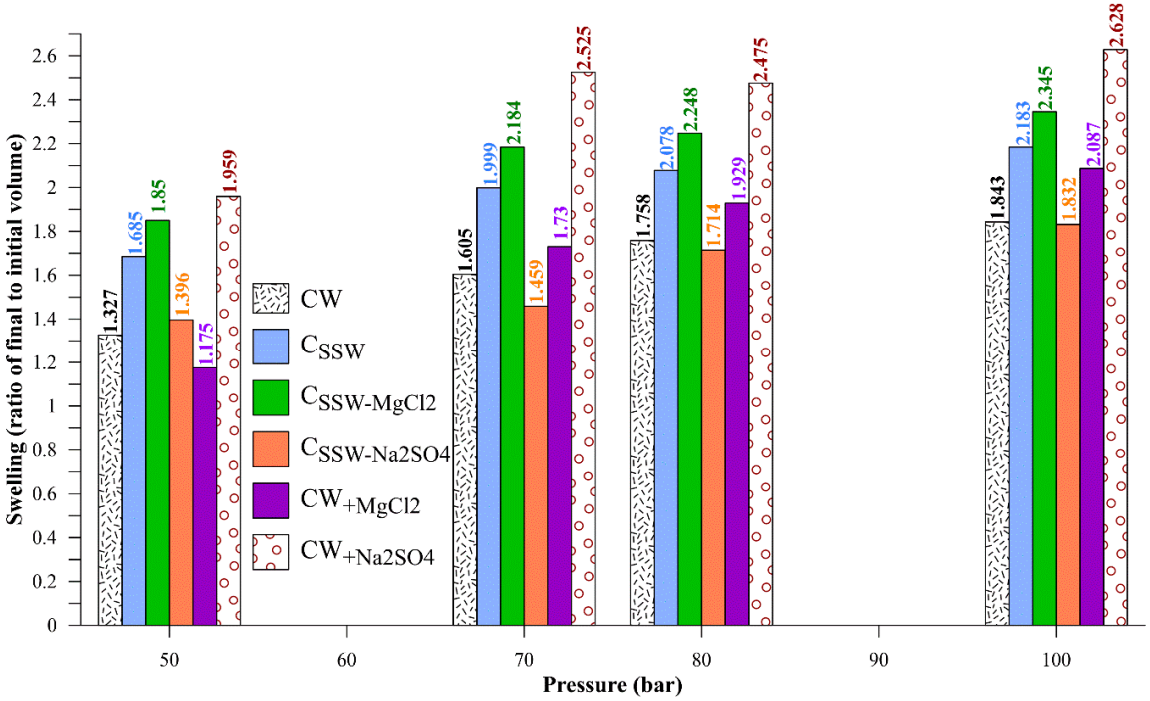

Figure 4. Swelling (ratio of final to initial volume) of the n-decane pendant for different carbonated brines for the pressure range of 50–100 bar at 45 °C.

Figure 5 shows the effective diffusion coefficient of CO_2 into n-decane from CB (C_{SSW}, $C_{SSW-MgCl2}$, $CW_{+Na2SO4}$, $C_{SSW-Na2SO4}$ and CW_{+MgCl2}) and CW for pressures 50, 70, 80, and 100 bar at 45 °C. Depending on the phase of CO_2 it may be observed that D_{CO2} is both directly and inversely proportional to pressure. For the gaseous CO_2, the D_{CO2} is inversely proportional to pressure, whereas when the CO_2 is supercritical, the D_{CO2} is directly proportional to the pressure; this observation was common for all the CB types. Similar observations were also made by [27]. Furthermore, it may be observed from Figure 5 that at isobaric conditions, in the presence of salt (CB) the D_{CO2} is well scattered above and below that of CW. Therefore, the presence of salt in CW both increases and decreases the rate of CO_2 mass transfer and is a function of the type of salt. The CB containing Na_2SO_4 ($CW_{+Na2SO4}$) and absence of $MgCl_2$ ($C_{SSW-MgCl2}$) showed a higher D_{CO2} than CW, while the CB containing $MgCl_2$ (CW_{+MgCl2}) and absence of Na_2SO_4 ($C_{SSW-Na2SO4}$) led to a lower diffusion coefficient than CW. The D_{CO2} was highest for $CW_{+Na2SO4}$, while the lowest was observed for CW_{+MgCl2}. On average (average over the pressure) approximately 57% increase in D_{CO2} for $CW_{+Na2SO4}$ was observed compared to CW_{+MgCl2}, and approximately 25% increase in D_{CO2} for $CW_{+Na2SO4}$ was observed compared to CW. The combination of Na_2SO_4+$MgCl_2$ (C_{SSW}) led to a reduction in D_{CO2} when compared to $CW_{+Na2SO4}$; however, it was higher than that of CW_{+MgCl2}. The D_{CO2} for C_{SSW} was marginally higher than that of CW.

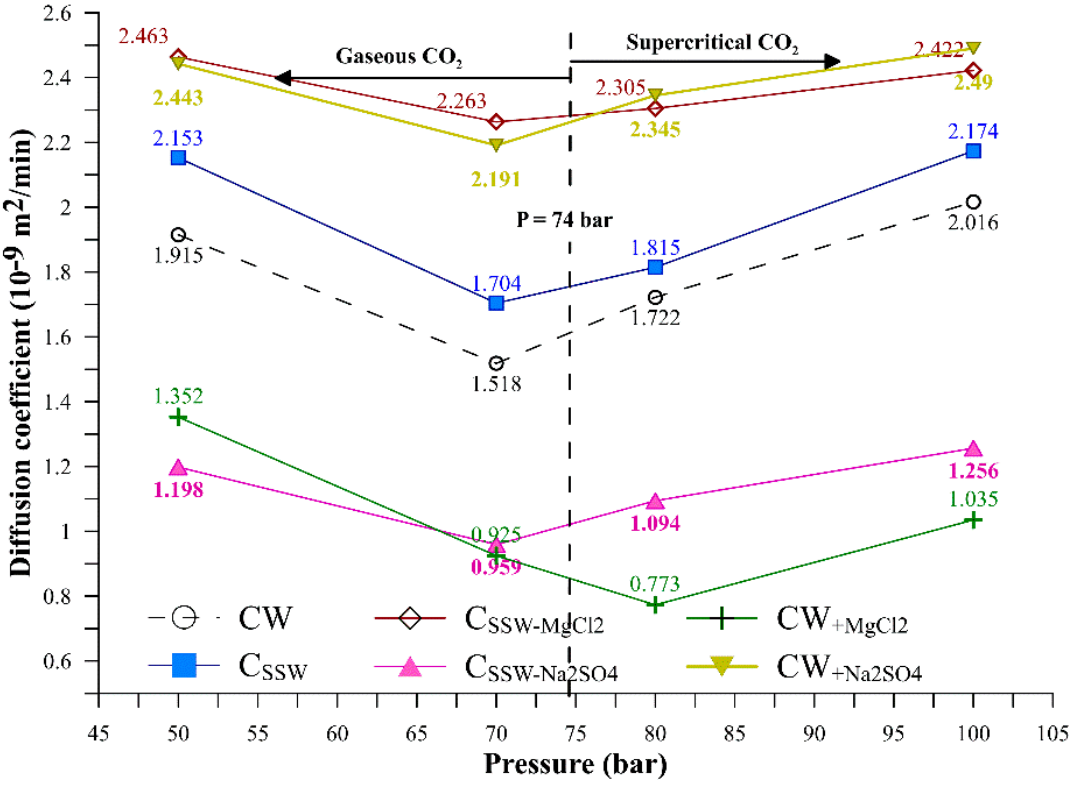

Figure 5. Effective diffusion coefficient of CO_2 into n-C10 from different CB and CW for pressures; 50, 70, 80, and 100 bar at 45 °C.

3.2. IFT

Table 3 shows the equilibrium IFT of brine/n-decane for different brine compositions along with their pH at 45 °C and different pressures. Table 3 shows that initial pH is approximately 7 ±0.2; after saturation of brines with CO_2 at the different pressures, the pH becomes approximately 3.0. The presence of salts in CW slightly alters the pH. IFT of DIW/n-decane (50.13 mN/m) compares well with literature (50.25 mN/m [47]). When brine C_{SSW}, $C_{SSW-Na2SO4}$, and CW_{+MgCl2} brines were used, they reduced IFT. The IFT reduction for CW_{+MgCl2} (36.5%) and $C_{SSW-Na2SO4}$ (30%), followed by C_{SSW} (13.8%). Whereas when brines $CW_{+Na2SO4}$ and $C_{SSW-MgCl2}$ were used the IFT increased by 4.9% and 2.1%, respectively.

Table 3. pH and IFT for different CB at 1, 50, 70, 80, and 100 bar at 45 °C.

Pressure (bar)	IFT (mN/m)					
	CW	C_{SSW}	$C_{SSW-MgCl2}$	$C_{SSW-Na2SO4}$	CW_{+MgCl2}	$CW_{+Na2SO4}$
1	50.13	43.18	51.19	31.09	31.82	52.58
50	56.45	54.35	57.31	35.26	32.28	57.95
70	63.90	63.80	67.50	47.85	40.5	62.75
80	62.67	60.49	58.14	50.85	51.97	60.18
100	52.43	50.46	49.56	46.56	30.26	49.73
Pressure (bar)	**pH**					
	CW	C_{SSW}	$C_{SSW-MgCl2}$	$C_{SSW-Na2SO4}$	CW_{+MgCl2}	$CW_{+Na2SO4}$
1	7.00	6.97	7.02	6.61	6.57	7.13
50	3.24	3.27	3.25	3.15	3.19	3.37
70	3.2	3.22	3.21	3.1	3.14	3.33
80	3.18	3.21	3.19	3.09	3.13	3.31
100	3.17	3.19	3.18	3.07	3.11	3.30

The dynamic IFTs are presented in Figure 6 for different pressures; 50 bar (6a), 70 bar (6b), 80 bar (6c), and 100 bar (6d) at 45 °C. The influence of CO_2-saturated brines on the dynamic IFT may be divided into two groups. For most of the pressures, the first group (increasing IFT trend) consists of brines C_{SSW}, $C_{SSW\text{-}MgCl2}$, $CW_{+Na2SO4,}$ and CW. The second group (decreasing IFT trend) shows that $C_{SSW\text{-}Na2SO4}$ and CW_{+MgCl2} reduce IFTs' profiles as a function of time. The IFT reduction occurs with brines containing $MgCl_2$ ($C_{SSW\text{-}Na2SO4}$ and CW_{+MgCl2}), with the highest reduction when the brine contains only $MgCl_2$ (CW_{+MgCl2}). Therefore, the presence of $MgCl_2$ in CW reduces the IFT with time until the equilibrium is reached, while the presence of Na_2SO_4 in CW increases the IFT. At all pressures, $MgCl_2$ in CW and C_{SSW} reduces the IFT. Marginal reduction of IFT (about 2 mN/m) for $C_{SSW\text{-}Na2SO4}$ brine at 100 bar. For better understanding the effect of brines on swelling, diffusion coefficient and IFT, the next section addresses the relation between the IFT and concentration of the diffused CO_2 into n-decane.

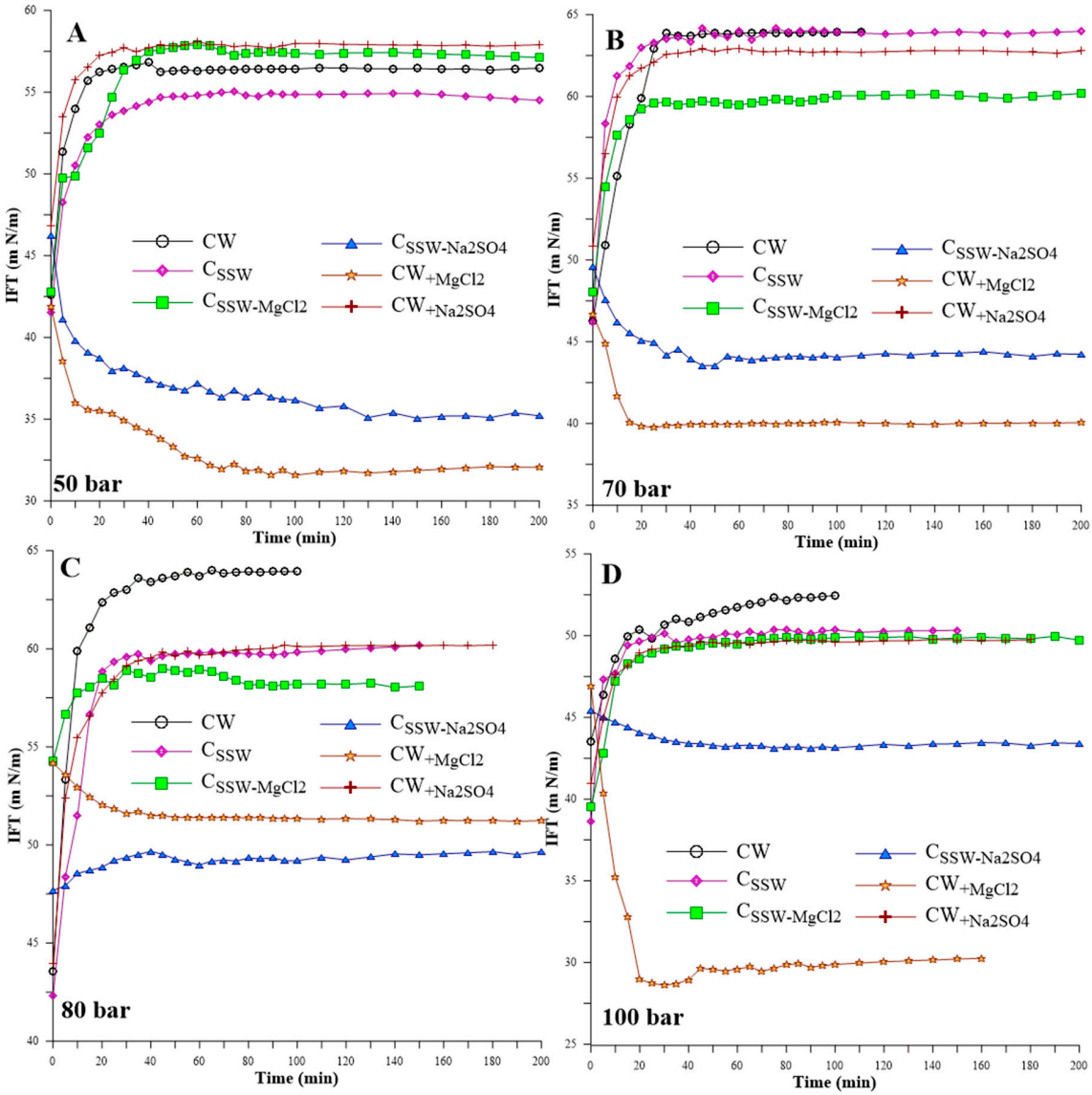

Figure 6. Dynamic changes in the CB/n-decane IFT for different brine compositions at 50 bar (**a**), 70 bar (**b**), 80 bar (**c**), and 100 bar (**d**) at 45 °C.

3.3. IFT and Concentration of Transferred CO_2 into n-Decane

Figure 7 shows the equilibrium concentration (10^{-6} mol/ml) of the CO_2-transferred CB into the n-decade drop against equilibrium IFT (m N/m). The IFT vs CO_2 concentration profiles in Figure 7 may be divided into two regions—higher and lower concentration regions. As shown, the higher concentration trends of the diffused CO_2 correspond to C_{SSW}, $C_{SSW\text{-}MgCl2}$, and $CW_{+Na2SO4}$ brines. The lower CO_2 concentration trends correspond to CW, $C_{SSW\text{-}Na2SO4}$, and CW_{+MgCl2}. CO_2 concentrations (low and high) for the different pressures are as follows; 50 bar ($5.7-8.5*10^{-7}$ and $2.1-2.3*10^{-6}$), 70 bar ($2.1-2.6*10^{-6}$ and $4.1-6.3*10^{-6}$), 80 bar ($4.5-5.0*10^{-6}$ and $5.9-8*10^{-6}$). CO_2 concentrations and the IFT trends are consistent with and support the conclusion where, in general at all the pressures, the presence of Na_2SO_4 increases the diffusion of CO_2, while the $MgCl_2$ reduces the IFT. For example, in Figures 3 and 4, Na_2SO_4 enhances the CO_2 mass transfer. Larger swelling of drop phase (n-decane) is also observed for cases where the brine contains Na_2SO_4 ($CW_{+Na2SO4}$), while lower swelling is observed for brine consisting of $MgCl_2$ (CW_{+MgCl2}). In other words, good correlations exist between the mass transfer trends (Figures 3 and 4) and the analytical data of the transferred CO_2 into n-decane (Figure 7), where the lowest diffusion coefficients are related to brines containing $MgCl_2$ ($C_{SSW\text{-}Na2SO4}$ and CW_{+MgCl2}) and the highest diffusion coefficients are related to brines containing Na_2SO_4 ($C_{SSW\text{-}MgCl2}$ and $CW_{+Na2SO4}$). The case of C_{SSW}, where it contains both salts ($MgCl_2$ and Na_2SO_4), shows that the diffusion coefficients are between the high ($CW_{+Na2SO4}$) and low (CW_{+MgCl2}). It is also interesting to see that SO_4^{2-} dominates the effect when co-present with Mg^{2+}.

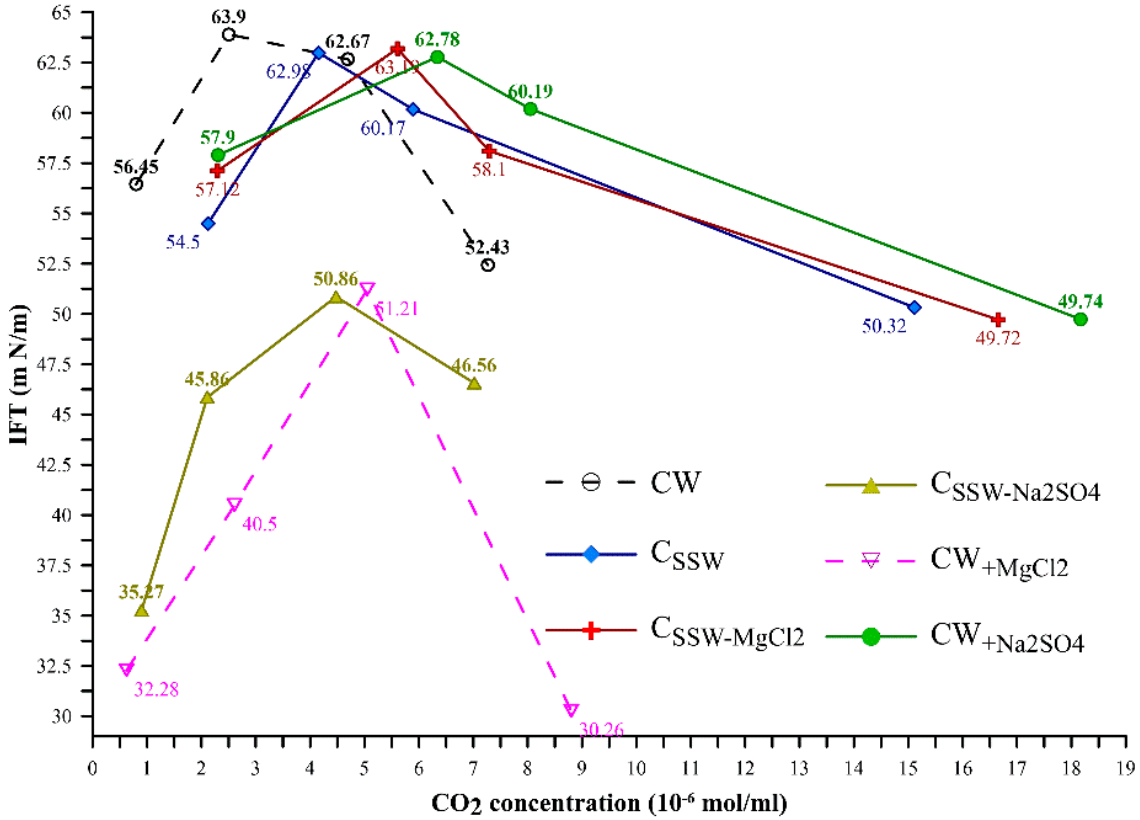

Figure 7. IFT as a function of CO_2 concentration in the n-decane.

3.4. Interfacial Adsorption Isotherm (Surface Excess)

The observed reduction alteration in IFT by SO_4^{2-} (Na_2SO_4) and Mg^{2+} ($MgCl_2$) ions may be related to the degree of hydration (number of water molecules surrounding an ion) and hydration energy/enthalpy. Among the major ions present in the SSW, Mg^{2-} ion has the smallest ionic radius (0.072 nm), compared to SO_4^{2-} (0.242 nm [2]) and CO_2 (232 nm). However, as a bivalent the Mg^{2-} ions

have high hydration energy. They therefore form tight bonds to the first hydration shell $[Mg(H_2O)_6]^{2+}$. Hence, they have a highly effective size leading to lesser adsorption and early saturation at the interface [48]. Higher hydration energy would also mean a higher affinity towards the CW/oil interface [29,49].

When Na_2SO_4 and $MgCl_2$ are combined as in C_{SSW}, the IFT reduction is intermediate between that of $CW_{+Na2SO4}$ and CW_{+MgCl2}. The formation of complexes of Mg^{2+} and Na^+ with $SO_4{}^{2-}$ due to the combination of Na_2SO_4 and $MgCl_2$ would reduce the free ions of Mg^{2+} and Na^+ [50]. Therefore, a lower concentration of Mg^{2+} would mean fewer ions being adsorbed at the CB/n-decane interface and hence, a smaller reduction in IFT. Accordingly, it was observed in Figure 6 and Table 3 that for C_{SSW} the IFT was intermediate between $CW_{+Na2SO4}$ and that of only composed of CW_{+MgCl2}. O'Brien, et al. [51] in their studies of hydration of $SO_4{}^{2-}$ ions, reported that they are surrounded by up to 14 hydration ions, where each hydrogen atom interacts with $SO_4{}^{2-}$ or the oxygen atom of another water molecule. Their studies indicated that the outer-shell water molecules have free OH [51]. It may be suggested that the possible mechanism where the local OH at the interface may slightly reduce the IFT, which then would promote the transportation of CO_2 into n-decane drop. This is in contrast to that for Mg^{2-} ions, where hydrated ions are tightly packed at the interface area, which resist the transportation of CO_2 across the interface and accumulate at the interface. It is interesting that the presence of both ions brings the equilibrium IFT into a level between the two the individual ions.

Figure 7 clearly illustrates and summarizes the brine interaction described above. It is shown that $C_{SSW\text{-}Na2SO4}$ and $C_{SSW+MgCl2}$ restrict the transfer of CO_2; however, they reduce the IFT of the system, compared to the other CBs, C_{SSW}, $C_{SSW\text{-}\,MgCl2}$ and $CW_{+Na2SO4}$.

4. Conclusions

The CO_2 mass transfer and the interfacial phenomena of CW/n-decane are the primary recovery mechanisms of CWI. The impact of salts on CO_2 mass transfer on IFT has rarely been investigated. The present work, through experimental and numerical methods, addresses the impact of $MgCl_2$ and Na_2SO_4 presence in carbonated water (CW) on the IFT of CW/n-decane and the mass transfer of CO_2. The experimental work was carried out for pressures between 50–100 bar and at 45 °C. The following conclusions were made from the analysis.

Mg^{2+} ion has shown to reduce both the CB/n-decane IFT (36.5%) and the diffusion coefficient of CO_2 into n-decane, in comparison with CW/n-decane system. It is suggested here that since Mg^{2+} has the smallest ionic radius (0.072 nm), and as a divalent ion it has high hydration energy. It therefore forms a tight bond to the first hydration shell $[Mg(H_2O)6]^{2+}$; accordingly, it has high effective size and when it adsorbs at the interface, it reduces the IFT. In the case of $SO_4{}^{2-}$, the ionic radius (0.242 nm) is larger than that of Mg^{2+} and has lower hydration energy than Mg^{2+}. Furthermore, it is reported that $SO_4{}^{2-}$ ion is surrounded by up to 14 hydration ions, where each hydrogen atom interacts with $SO_4{}^{2-}$ or the oxygen atom of another water molecule, indicating that the outer-shell water molecules have free OH groups. It is suggested here that a possible mechanism where the local OH groups at the interface may lightly and locally reduce IFT, which then promote the transportation of CO_2 into n-decane drop. The suggested mechanisms for both ions are supported by observation, where in the dynamic IFT, the equilibrium is reached faster in case of Mg^{2+} compared to that with $SO_4{}^{2-}$.

Brine effects on altering carbonated water physical processes such as diffusion and IFT have been identified. Moreover, the contribution and proposed mechanisms of the different ions ($SO_4{}^{2-}$ and Mg^{2+}) to the physical process in carbonated water/hydrocarbon have been addressed, which contribute to EOR.

Author Contributions: Conceptualization, A.A.H. and N.B.; Methodology, A.A.H. and N.B.; Software, N.B.; Validation, N.B.; Formal Analysis, A.A.H. and N.B.; Investigation, A.A.H. and N.B.; Resources, A.A.H. and N.B.; Data Curation, N.B.; Writing-Original Draft Preparation, A.A.H. and N.B.; Writing-Review & Editing, A.A.H. and N.B.; Visualization, A.A.H. and N.B.; Supervision, A.A.H.

Funding: This research received no external funding.

Acknowledgments: The authors would like to thank the support of department engineers, Department of Energy and Petroleum Engineering, UiS.

Conflicts of Interest: The authors declare no conflict of interest.

References

1. Riazi, M.; Sohrabi, M.; Jamiolahmady, M.; Ireland, S. Oil recovery improvement using CO_2-enriched water injection. In Proceedings of the 2009 EUROPEC/EAGE Conference and Exhibition, Amsterdam, The Netherlands, 8–11 June 2009.
2. Esene, C.; Rezaei, N.; Aborig, A.; Zendehboudi, S. Comprehensive review of carbonated water injection for enhanced oil recovery. *Fuel* **2019**, *237*, 1086–1107. [CrossRef]
3. Kechut, N.I.; Sohrabi, M.; Jamiolahmady, M. Experimental and numerical evaluation of carbonated water injection (cwi) for improved oil recovery and CO_2 storage. In Proceedings of the 2011 SPE EUROPEC/EAGE Annual Conference and Exhibition, Vienna, Austria, 23–26 May 2011.
4. Riazi, M.; Sohrabi, M.; Jamiolahmady, M. Experimental study of pore-scale mechanisms of carbonated water injection. *Transp. Porous Media* **2011**, *86*, 73–86. [CrossRef]
5. Dejam, M.; Hassanzadeh, H. Diffusive leakage of brine from aquifers during CO_2 geological storage. *Adv. Water Resour.* **2018**, *111*, 36–57. [CrossRef]
6. Dejam, M.; Hassanzadeh, H. The role of natural fractures of finite double-porosity aquifers on diffusive leakage of brine during geological storage of CO_2. *Int. J. Greenh. Gas Control* **2018**, *78*, 177–197. [CrossRef]
7. Nowrouzi, I.; Manshad, A.K.; Mohammadi, A.H. Effects of dissolved binary ionic compounds and different densities of brine on interfacial tension (ift), wettability alteration, and contact angle in smart water and carbonated smart water injection processes in carbonate oil reservoirs. *J. Mol. Liquids* **2018**, *254*, 83–92. [CrossRef]
8. Mashayekhizadeh, V.; Kord, S.; Dejam, M. Eor potential within iran. *Spec. Top. Rev. Porous Media Int. J.* **2014**, *5*, 325–354. [CrossRef]
9. Gomari, K.R.; Hamouda, A. Effect of fatty acids, water composition and ph on the wettability alteration of calcite surface. *J. Pet. Sci. Eng.* **2006**, *50*, 140–150. [CrossRef]
10. Zhang, P.; Tweheyo, M.T.; Austad, T. Wettability alteration and improved oil recovery by spontaneous imbibition of seawater into chalk: Impact of the potential determining ions Ca^{2+}, Mg^{2+}, and SO_4^{2-}. *Colloids Surf. A Physicochem. Eng. Asp.* **2007**, *301*, 199–208. [CrossRef]
11. Manshad, A.K.; Nowrouzi, I.; Mohammadi, A.H. Effects of water soluble ions on wettability alteration and contact angle in smart and carbonated smart water injection process in oil reservoirs. *J. Mol. Liquids* **2017**, *244*, 440–452. [CrossRef]
12. Hamouda, A.A.; Rezaei Gomari, K.A. Influence of temperature on wettability alteration of carbonate reservoirs. In Proceedings of the 2006 SPE/DOE Symposium on Improved Oil Recovery, Tulsa, OK, USA, 22–26 April 2006.
13. Cai, B.-Y.; Yang, J.-T.; Guo, T.-M. Interfacial tension of hydrocarbon+ water/brine systems under high pressure. *J. Chem. Eng. Data* **1996**, *41*, 493–496. [CrossRef]
14. Lashkarbolooki, M.; Ayatollahi, S. Investigation of ionic liquids based on pyridinium and imidazolium as interfacial tension reducer of crude oil-water and their synergism with mgcl2. *J. Pet. Sci. Eng.* **2018**, *171*, 414–421. [CrossRef]
15. Manshad, A.K.; Olad, M.; Taghipour, S.A.; Nowrouzi, I.; Mohammadi, A.H. Effects of water soluble ions on interfacial tension (ift) between oil and brine in smart and carbonated smart water injection process in oil reservoirs. *J. Mol. Liquids* **2016**, *223*, 987–993. [CrossRef]
16. Serrano-Saldaña, E.; Domínguez-Ortiz, A.; Pérez-Aguilar, H.; Kornhauser-Strauss, I.; Rojas-González, F. Wettability of solid/brine/n-dodecane systems: Experimental study of the effects of ionic strength and surfactant concentration. *Colloids Surf. A Physicochem. Eng. Asp.* **2004**, *241*, 343–349. [CrossRef]
17. Ikeda, N.; Aratono, M.; Motomura, K. Thermodynamic study on the adsorption of sodium chloride at the water/hexane interface. *J. Colloid Interface Sci.* **1992**, *149*, 208–215. [CrossRef]
18. Aveyard, R.; Saleem, S.M. Interfacial tensions at alkane-aqueous electrolyte interfaces. *J. Chem. Soc. Faraday Trans. 1 Phys. Chem. Condens. Phases* **1976**, *72*, 1609–1617. [CrossRef]

19. Lashkarbolooki, M.; Ayatollahi, S.; Riazi, M. The impacts of aqueous ions on interfacial tension and wettability of an asphaltenic–acidic crude oil reservoir during smart water injection. *J. Chem. Eng. Data* **2014**, *59*, 3624–3634. [CrossRef]
20. Hosseini, S.; Shuker, M.; Hosseini, Z.; Tomocene, T.J.; Shabib-Asl, A.; Sabet, M. The role of salinity and brine ions in interfacial tension reduction while using surfactant for enhanced oil recovery. *Res. J. Appl. Sci. Eng. Technol.* **2015**, *9*, 722–726. [CrossRef]
21. Badakshan, A.; Bakes, P. *The Influence of Temperature and Surfactant Concentration on Interfacial Tension of Saline Water and Hydrocarbon Systems in Relation to Enhanced Oil Recovery by Chemical Flooding*; Society of Petroleum Engineers: Richardson, TX, USA, 1990.
22. Isdahl, O.M. *Influence of Silica Based Nanofluid on the Physical Properties, Ift, and CO_2 Diffusion in a Carbonated Water-n-Decane System: An Experimental and Numerical Study*; University of Stavanger: Stavanger, Norway, 2017.
23. Perera, M.; Gamage, R.; Rathnaweera, T.; Ranathunga, A.; Koay, A.; Choi, X. A review of CO_2-enhanced oil recovery with a simulated sensitivity analysis. *Energies* **2016**, *9*, 481. [CrossRef]
24. Shi, Y.; Zheng, S.; Yang, D. Determination of individual diffusion coefficients of alkane solvent (s)–CO_2–heavy oil systems with consideration of natural convection induced by swelling effect. *Int. J. Heat Mass Transf.* **2017**, *107*, 572–585. [CrossRef]
25. Yang, D.; Gu, Y. Determination of diffusion coefficients and interface mass-transfer coefficients of the crude oil−CO_2 system by analysis of the dynamic and equilibrium interfacial tensions. *Ind. Eng. Chem. Res.* **2008**, *47*, 5447–5455. [CrossRef]
26. Yang, C.; Gu, Y. New experimental method for measuring gas diffusivity in heavy oil by the dynamic pendant drop volume analysis (dpdva). *Ind. Eng. Chem. Res.* **2005**, *44*, 4474–4483. [CrossRef]
27. Yang, D.; Tontiwachwuthikul, P.; Gu, Y. Dynamic interfacial tension method for measuring gas diffusion coefficient and interface mass transfer coefficient in a liquid. *Ind. Eng. Chem. Res.* **2006**, *45*, 4999–5008. [CrossRef]
28. Bagalkot, N.; Hamouda, A.A. Diffusion coefficient of CO_2 into light hydrocarbons and interfacial tension of carbonated water–hydrocarbon system. *J. Geophys. Eng.* **2018**, *15*, 2516. [CrossRef]
29. Zhu, H.; Shanks, B.H.; Heindel, T.J. Effect of electrolytes on co−water mass transfer. *Ind. Eng. Chem. Res.* **2009**, *48*, 3206–3210. [CrossRef]
30. Collins, K.D. Charge density-dependent strength of hydration and biological structure. *Biophys. J.* **1997**, *72*, 65–76. [CrossRef]
31. Nguyen, T.; Ali, S. Effect of nitrogen on the solubility and diffusivity of carbon dioxide into oil and oil recovery by the immiscible wag process. *J. Can. Pet. Technol.* **1998**, *37*. [CrossRef]
32. Sigmund, P.M. Prediction of molecular diffusion at reservoir conditions. Part 1-measurement and prediction of binary dense gas diffusion coefficients. *J. Can. Pet. Technol.* **1976**, *15*. [CrossRef]
33. Upreti, S.R.; Mehrotra, A.K. Diffusivity of CO_2, CH_4, C_2H_6 and N_2 in athabasca bitumen. *Can. J. Chem. Eng.* **2002**, *80*, 116–125. [CrossRef]
34. Sheikha, H.; Pooladi-Darvish, M.; Mehrotra, A.K. Development of graphical methods for estimating the diffusivity coefficient of gases in bitumen from pressure-decay data. *Energy Fuels* **2005**, *19*, 2041–2049. [CrossRef]
35. Riazi, M.R. A new method for experimental measurement of diffusion coefficients in reservoir fluids. *J. Pet. Sci. Eng.* **1996**, *14*, 235–250. [CrossRef]
36. Bagalkot, N.; Hamouda, A.A. Experimental and numerical method for estimating diffusion coefficient of the carbon dioxide into light components. *Ind. Eng. Chem. Res.* **2017**, *56*, 2359–2374. [CrossRef]
37. Yang, D.; Tontiwachwuthikul, P.; Gu, Y. Interfacial tensions of the crude oil+ reservoir brine+ CO_2 systems at pressures up to 31 MPa and temperatures of 27 °C and 58 °C. *J. Chem. Eng. Data* **2005**, *50*, 1242–1249. [CrossRef]
38. Ghorbani, M.; Mohammadi, A.H. Effects of temperature, pressure and fluid composition on hydrocarbon gas-oil interfacial tension (ift): An experimental study using adsa image analysis of pendant drop test method. *J. Mol. Liquids* **2017**, *227*, 318–323. [CrossRef]
39. Hamouda, A.A.; Maevskiy, E. Oil recovery mechanism (s) by low salinity brines and their interaction with chalk. *Energy Fuels* **2014**, *28*, 6860–6868. [CrossRef]

40. Lemmon, E.; McLinden, M.; Friend, D.; Linstrom, P.; Mallard, W. *Nist Chemistry Webbook, Nist Standard Reference Database Number 69*; National Institute of Standards and Technology: Gaithersburg, MD, USA, 2011.
41. Duan, Z.; Sun, R. An improved model calculating CO_2 solubility in pure water and aqueous nacl solutions from 273 to 533 k and from 0 to 2000 bar. *Chem. Geol.* **2003**, *193*, 257–271. [CrossRef]
42. Bagalkot, N.; Hamouda, A.A.; Isdahl, O.M. Dynamic interfacial tension measurement method using axisymmetric drop shape analysis. *MethodsX* **2018**, *5*, 676–683. [CrossRef] [PubMed]
43. Gmb, K. Drop Shape Analyzer—dsa100 hp. Available online: https://www.kruss-scientific.com/fileadmin/user_upload/website/brochures/kruss-techdata-dsa100hp-en.pdf (accessed on 29 May 2018).
44. Jaeger, P.T.; Eggers, R. Interfacial properties at elevated pressures in reservoir systems containing compressed or supercritical carbon dioxide. *J. Supercrit. Fluids* **2012**, *66*, 80–85. [CrossRef]
45. Bagalkot, N.; Hamouda, A.A. Interfacial tension and CO_2 diffusion coefficients for a CO_2+ water and n-decane system at pressures of 10 to 160 bar. *RSC Adv.* **2018**, *8*, 38351–38362. [CrossRef]
46. Jamialahmadi, M.; Emadi, M.; Müller-Steinhagen, H. Diffusion coefficients of methane in liquid hydrocarbons at high pressure and temperature. *J. Pet. Sci. Eng.* **2006**, *53*, 47–60. [CrossRef]
47. Yang, C.; Gu, Y. Diffusion coefficients and oil swelling factors of carbon dioxide, methane, ethane, propane, and their mixtures in heavy oil. *Fluid Phase Equilib.* **2006**, *243*, 64–73. [CrossRef]
48. Zeppieri, S.; Rodríguez, J.; López de Ramos, A. Interfacial tension of alkane+ water systems. *J. Chem. Eng. Data* **2001**, *46*, 1086–1088. [CrossRef]
49. Brandal, Ø.; Sjöblom, J.; Øye, G. Interfacial behavior of naphthenic acids and multivalent cations in systems with oil and water. I. A pendant drop study of interactions between n-dodecyl benzoic acid and divalent cations. *J. Dispers. Sci. Technol.* **2004**, *25*, 367–374. [CrossRef]
50. Garrels, R.; Thompson, M. A chemical model for sea water at 25 °C and one atmosphere total pressure. *Am. J. Sci.* **1962**, *260*, 57–66. [CrossRef]
51. O'Brien, J.T.; Prell, J.S.; Bush, M.F.; Williams, E.R. Sulfate ion patterns water at long distance. *J. Am. Chem. Soc.* **2010**, *132*, 8248–8249. [CrossRef] [PubMed]